ANNULAR ULTRASONIC MICROMOTORS FABRICATED FROM BULK PZT

Prakruthi Hareesh and Don L. DeVoe
University of Maryland, College Park, USA

ABSTRACT

This paper reports a new class of bulk PZT traveling wave ultrasonic micromotor fabricated from a single sheet of bulk PZT. Actuation of electrode pairs in a differential quadrature configuration is enabled by use of transverse interdigitated electrodes to achieve bending-mode actuation of a stator ring, enabling a simple single-layer device design and enhancing the effective input voltage applied to the device. Using fabricated micromotor patterned by micro powder blasting, bi-directional rotary motion of 100 µm thick glass rotors is successfully demonstrated.

INTRODUCTION

Small-scale traveling wave ultrasonic motors are attractive for applications such as camera autofocal lenses, ultrasound catheters systems and miniature robotics due to their ability to produce high torques at low speeds, without the requirement of gears. At the meso- and micro-scale, they have several advantages over their electromagnetic and electrostatic counterparts such as ease of fabrication, high dielectric constant and lower operating voltages.

There has been a lot of work in the field of traveling wave ultrasonic motors since its invention by Sashida [1] in 1983, which was commercialized for use in camera auto-focus mechanisms. Since the introduction of this first traveling wave motor design, a range of millimeter scale ultrasonic motors based on the same principles have been explored. Flynn reported the first millimeter scale traveling wave motors using both thin film and bulk PZT [2], but only uni-directional rotation was demonstrated and further miniaturization was not possible due to fabrication process limitations. While various traveling wave ultrasonic motors have been reported using conventional microfabrication techniques and thin film piezoelectric materials [3-6], these devices have relied on complex fabrication processes involving multiple deposition, photolithography, and etching steps. Furthermore, because these motors typically employ thin film piezoelectric materials for actuation, their achievable power densities and output torques are limited, making them inappropriate for many practical applications.

In this work, we demonstrate a miniaturized traveling wave ultrasonic motor employing a stator fabricated from a single sheet of bulk PZT and requiring only two photolithography steps, greatly simplifying their design and manufacture while improving device performance and microfabrication costs. Using the validated fabrication process, stator performance is characterized and the operation of millimeter-scale motors is demonstrated, with a bi-directional rotor motion at stable rotor speeds as low as 30 rpm achieved.

FABRICATION

Micromotor stators have been successfully fabricated using a combination of chem-mechanical polishing, dry film photolithography, micro powder blasting (MPB) of a bulk PZT sheet, and lift-off metallization, as shown in Figure 1. A micro powder blasting process, described in our previous work [7-8], was used to fabricate bulk PZT stators in a 127 µm thick sheet of PZT 5A4E, and 100 µm thick glass rotors having the same diameter as that of stator rings were fabricated by a single lithography step using the same MPB etching technique. A typical stator fabricated in this process is shown in Figure 2.

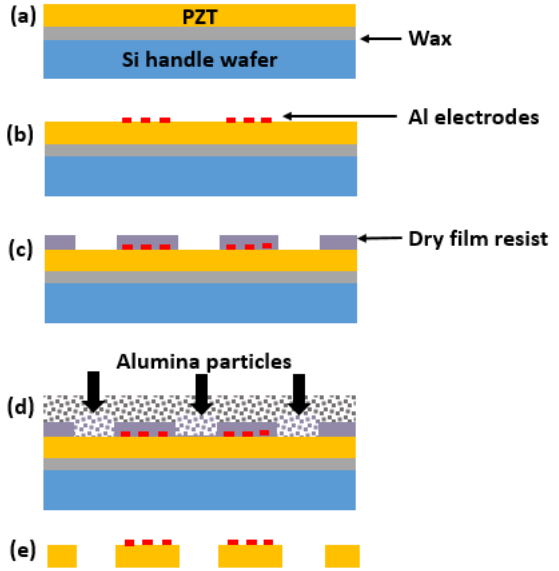

Figure 1: Bulk PZT micromotor fabrication process, comprising (a) Bond PZT to a silicon substrate using wax, (b) deposition and patterning of Al electrodes (mask 1), (c) Laminate and pattern dry film resist to define stator geometry (mask 2), (d) MPB to etch through Bulk PZT, (e) resist strip and release the stators.

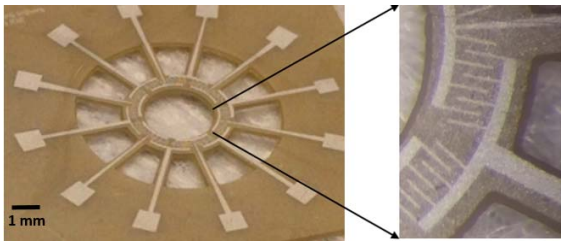

Figure 2: Bulk PZT stator (4 mm outer diameter & ring width of 600 µm), and magnified view of the transverse interdigitated electrodes (right) used for device actuation.

OPERATING PRINCIPLE

Traveling wave ultrasonic motors operate through the propagation of elastic waves which generate high-frequency elliptical motions with submicron amplitudes at the stator surface. The retrograde trajectories of particles

at the stator surface transfer momentum to a frictionally-coupled rotor as shown in Figure 3.

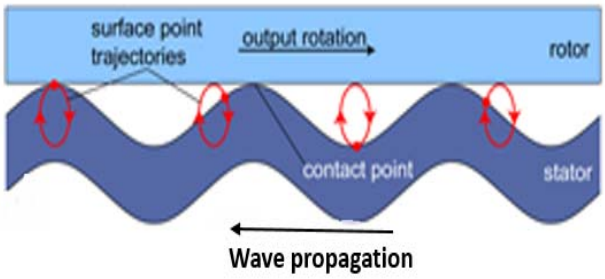

Figure 3: Stator surface points follow elliptical paths, with momentum transfer to a coupled stator in the opposite direction of wave propagation.

These motors employ piezoelectric materials which generate a strain due to an applied electric field, thereby generating these elastic waves. The traveling waves are generated by simultaneously exciting two standing waves by superimposing periodic inputs phase-shifted by a quarter wavelength in both time and space.

Based on the electrode design, piezoelectric actuators can be operated in d_{31} mode in which, when an electric field (E_3) is applied across the thickness of the piezoelectric film, a longitudinal strain (S_1) is generated within the film through the transverse d_{31} coupling coefficient following the constitutive relationship given by

$$S_1 = d_{31}E_3 \quad (1)$$

It can also be operated in d_{33} mode, wherein an actuation voltage applied between the electrodes generates field lines parallel to the fixed dipoles, resulting in longitudinal strain (S_3) though the d_{33} converse piezoelectric effect as

$$S_3 = d_{33}E_3 \quad (2)$$

From the perspective of electromechanical coupling, the use of longitudinal-mode d_{33} actuation ensures better device performance, since d_{31} is typically two to three times smaller than the d_{33} coupling coefficient.

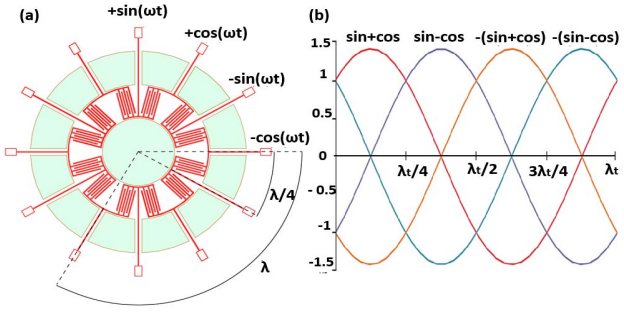

Figure 4: (a) Schematic of a B_{03} annular stator driven in differential quadrature, and (b) one cycle of differential signals applied to adjacent electrodes.

The devices use a transverse interdigitated electrode (TIE) design for PZT actuation, enabling out-of-plane bending actuation of the homogeneous piezoelectric stator using a set of alternating electrodes forming a series of capacitive gaps positioned along the length of the beam. After metallization, the PZT is re-poled along electric field lines between adjacent electrode pairs. TIE actuation also enables a novel drive scheme for ultrasonic micromotors termed differential quadrature drive (DQD).

A schematic of a B_{03} mode annular disk stator driven using DQD in shown in Figure 4a. Four sinusoidal drive signals are applied to the electrodes with each adjacent pair in quadrature, i.e. a temporal phase difference of a quarter wavelength between each adjacent signal (±sin, ±cos). Because the piezoelectric elements are excited by the difference between the adjacent signals (Figure 4b) that are in both temporal and spatial quadrature, the resulting B_{03} mode excitation generates a propagating traveling wave. The B_{03} mode was chosen to have three points of contact for the rotor for stable rotation.

EXPERIMENTAL RESULTS

Determination of B_{03} mode

In order to select the frequency corresponding to the B_{03} mode, a 0-5 V white noise signal was applied to a pair of electrodes using a waveform generator, and the response was measured using a Polytec laser doppler vibrometer (LDV). A Fourier transform was performed on this data to determine the frequencies of greatest amplitude. These frequencies were then isolated and examined to determine the resonant frequency corresponding to the desired mode shape. The B_{03} mode frequency for the ring stator tested was 54 KHz. This was repeated for all twelve electrode pairs and the difference in the B_{03} mode resonant frequencies between them was less than 2%, which can be attributed to slight variations in the geometry resulting from powder blasting. Figure 5 represents the eigenfrequency analysis of the stator using a finite element modeling software (COMSOL) highlighting the three circumferential nodes which constitute a B_{03} mode.

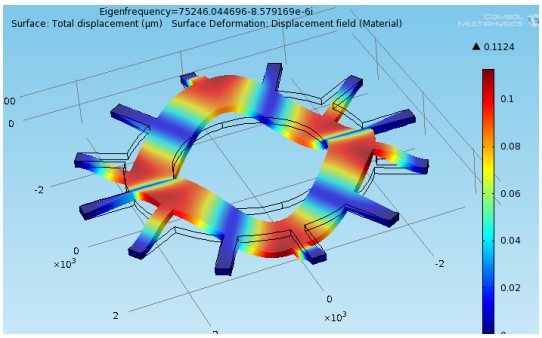

Figure 5: B_{03} mode (3 circumferential nodes and 0 radial nodes) of a 4 mm stator with a tether length of 1 mm simulated using COMSOL

Generation of standing waves and DQD actuation

Each electrode pair was actuated with a sine wave at the corresponding B_{03} mode frequency to generate standing waves. The TIE design enables the DQD scheme in which the electrode pairs can be actuated with a Sine-cosine signal instead of Sine-ground signal. This results in a √2x increase in the actuation voltage based on the design alone. Figure 6 shows a linear increase in the standing wave amplitudes with increasing voltages up to 80 V, which is the initial depolarizing voltage for PZT 5A4E. It can be seen that the DQD actuation results in standing wave amplitudes which are about 1.3x higher than when actuated with a sine-ground signal.

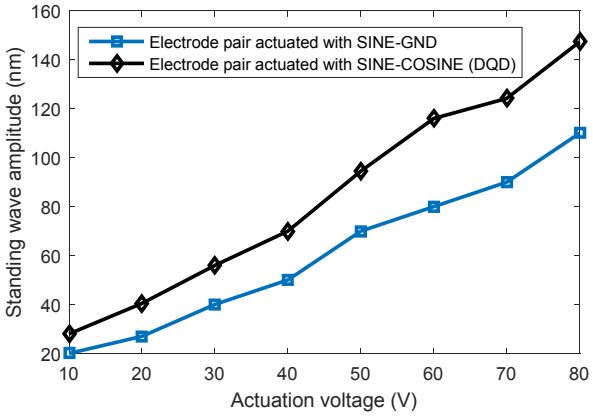

Figure 6: Standing wave amplitude response for one section of a 4 mm diameter stator with increasing actuation voltages showing √2 X increase in performance resulting from the DQD actuation scheme.

Stator Poling

The commercial PZT sheets are poled along the thickness of the material. In order to operate it in the d_{33} mode, the stators are first depolarized by heating to Curie temperature. Poling is then performed at a temperature of 100º C at 4 V/µm for 30 minutes and cooling it down to room temperature while maintaining the electric field at 4 V/µm. Each electrode pair is poled individually and successful poling is obtained when the standing wave amplitude after poling is higher than before poling.

Generation of traveling wave

The traveling waves are generated by applying four sinusoidal drive signals to the electrodes with each adjacent pair in quadrature (±sin, ±cos). Laser Doppler vibrometry was used to optically measure and track the traveling wave. The electrode pairs were actuated using sine, cosine, -sine and -cosine signals at the B_{03} mode resonant frequency to obtain a traveling wave. Sequential measurements from a 4 mm diameter stator at 54 kHz are shown in Figure 7. Bidirectional rotation of the traveling waves was obtained by reversing the order of input voltages. The stator traveling wave amplitude was measured all the way up to 80 V, the initial depolarizing field for the given electrode spacing. Traveling waves can be generated by actuating just one section (4 electrode pairs), two sections (8 electrode pairs) or all three sections (12 electrode pairs) as shown in Figure 8. The PZT stators exhibit nonlinear behavior when larger strains are generated. In our devices, a nonlinear increase in the traveling wave amplitudes beyond 200 nm, as can be seen in the figure.

Rotor motion

Glass disk rotors (4 mm diameter) were placed on top of the stators with no additional pre-load (Figure 9). Initial rotor vibration was observed at traveling wave amplitudes close to 200 nm. At about 200 nm of traveling wave amplitude, a stable rotor speed, opposite to the direction of traveling wave, was observed to be 30 rpm. By reversing the direction of the traveling wave, bi-directional rotation of the rotor was achieved. The rotor speed was found to non-linearly increase with increasing input voltages.

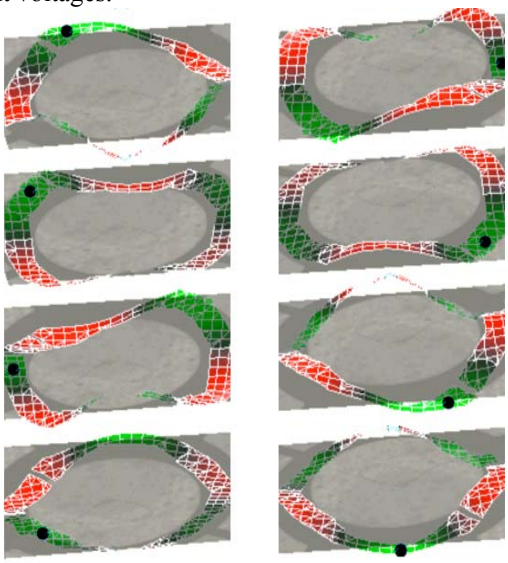

Figure 7: Scanning LDV measurements of a B_{03} traveling wave in a 4 mm diameter bulk PZT ring stator driven with TIE electrodes. The black dot shown traces the traveling wave propagation both anti-clockwise (left) and clockwise (right)

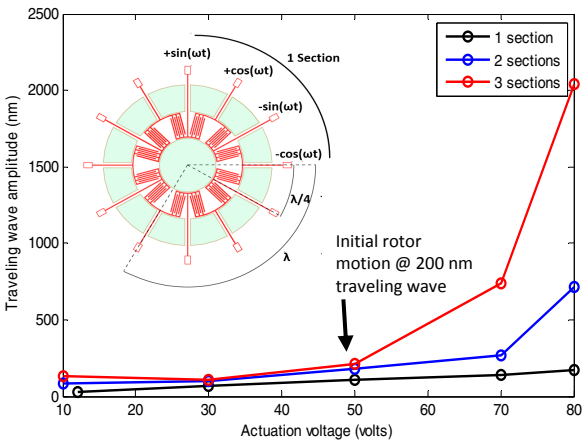

Figure 8: Traveling wave amplitude response with increasing voltages when one, two and all three sections are actuated, exhibiting non-linear behavior at high amplitudes. A wave amplitude of 200 nm is sufficient for bidirectional driving of a glass rotor at +/-50 V input.

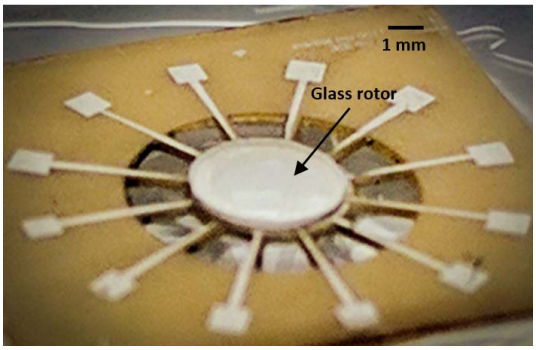

Figure 9: An assembled PZT stator - glass rotor device

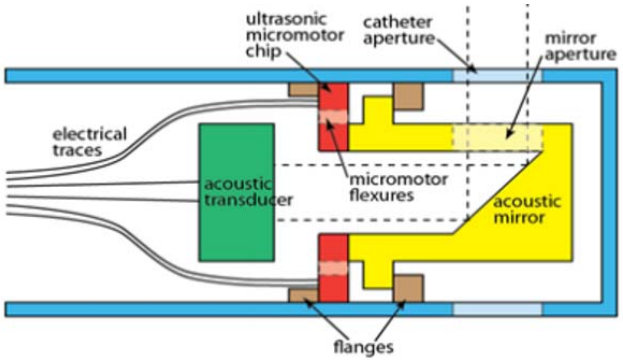

Figure 10: Schematic of an annular ultrasonic micromotor integrated into an intravascular ultrasound catheter tip.

CONCLUSION AND FUTURE WORK

In the recent times, ultrasonic micromotors have garnered significant interest in the field of medical robotics, such as imaging catheters. These catheters typically employ a flexible steel drive shaft to transfer torque from an external motor to the imaging probe, enabling 360º scanning around the probe circumference [9]. Ultrasonic motors are attractive as they eliminate the need for a mechanical drive shaft for probe rotation, significantly reducing catheter stiffness and thus enhancing steering control, improving image quality, and enabling arbitrary probe positioning for high resolution imaging of selected tissue regions.

This work has demonstrated successful miniaturization of ultrasonic bulk PZT traveling wave motors manufactured from a single sheet of PZT using a simple, low-cost approach. Bidirectional rotor motion with stable speeds as low as 30 rpm has been demonstrated for glass rotors with no applied pre-load. With applied normal force, these motors are expected to provide useful torque suitable for applications such as imaging catheters.

Preliminary work integrating the bulk PZT stator and an acoustic micro-mirror rotor for imaging has been carried out as shown in Figure 10. Future work would involve detailed rotor characterization and further miniaturization of these motors down to 1 mm diameter, enabling their integration into a functional intravascular ultrasound catheter tip.

ACKNOWLEDGEMENTS

The authors would like to thank the Vibrations Laboratory, University of Maryland, for providing access to the scanning Laser Doppler Vibrometer.

REFERENCES

[1] T. Sashida, T. Kenjo, *An Introduction to Ultrasonic Motors,* New York, NY, USA: Oxford Univ. Press, 2003, pp. 5–12.

[2] A. M. Flynn et al., “Piezoelectric micromotors for microrobots,” *J. Microelectromech. Syst*., vol. 1, no. 1, pp. 44–51, Mar. 1992.

[3] S. Piratla, M. Pandey, A. Lal, “Nanogap ultrasonic actuator for non-contact control of levitated inertial sensor rotor,” in *Proc. Solid-State Sens., Actuators, Microsyst. Workshop, Hilton Head*, SC, USA, Jun. 2012, pp. 82–85.

[4] R.Q. Rudy, G.L. Smith, D.L. DeVoe, G. Polcawich, “Millimeter-Scale Traveling Wave Rotary ultrasonic motors, *J. Microelectromech Syst.*, vol. 24, pp. 108-114, 2015.

[5] T. Kanda, A. Makino, T. Ono, K. Suzumori, T. Morita, M.K. Kurosawa, “A micro ultrasonic motor using a micro-machined bulk PZT transducer,” *Sensors and Actuators A*, 127, 131-138, 2006.

[6] S. Dong, S. P. Lim, K. H. Lee, J. Zhang, L. C. Lim and K. Uchino, "Piezoelectric ultrasonic micromotor with 1.5 mm diameter," in *IEEE Transactions on Ultrasonics, Ferroelectrics, and Frequency Control*, vol. 50, no. 4, pp. 361-367, April 2003.

[7] I. Misri, P. Hareesh, S. Yang, and D. L. DeVoe, “Microfabrication of bulk PZT transducers by dry film photolithography and micro powderblasting,” *J. Micromech. Microeng.*, vol. 22, no. 8, pp. 85017–85026, Aug. 2012.

[8] P. Hareesh, I. Misri, S. Yang, D.L. DeVoe, "Transverse interdigitated electrode actuation of homogeneous bulk PZT," *J. Microelectromech Syst*., 21, 1513-1518, 2012.

[9] S. Sharma, G. Gulati, “Current trends and future applications of intravascular ultrasound,” *Indian J. Radiol. Imaging*, vol. 13, no. 1, p. 53, Feb. 2003.

CONTACT

*D.L. DeVoe, Tel: +1-301-405-8125; ddev@umd.edu